Statistical mechanics of tuned cell signalling: sensitive collective response by synthetic biological circuits

M. Voliotis[1,2] **and T.B. Liverpool**[3,4]

[1] College of Engineering, Mathematics and Physical Sciences, University of Exeter, Exeter EX4 4QF, UK

[2] Centre for Predictive Modelling in Healthcare, University of Exeter, RILD Building, Exeter EX2 5DW, UK

[3] School of Mathematics, University of Bristol, University Walk, Bristol BS8 1TW, UK

[4] BrisSynBio, Life Sciences Building, Tyndall Avenue, Bristol BS8 1TQ, UK

Abstract. Living cells sense and process environmental cues through noisy biochemical mechanisms. This apparatus limits the scope of engineering cells as viable sensors. Here, we highlight a mechanism that enables robust, population-wide responses to external stimulation based on cellular communication, known as quorum sensing. We propose a synthetic circuit consisting of two mutually repressing quorum sensing modules. At low cell densities the system behaves like a genetic toggle switch, while at higher cell densities the behaviour of nearby cells is coupled via diffusible quorum sensing molecules. We show by systematic coarse graining that at large length and timescales that the system can be described using the Ising model of a ferromagnet. Thus, in analogy with magnetic systems, the sensitivity of the population-wide response, or its 'susceptibility' to a change in the external signal, is highly enhanced for a narrow range of cell-cell coupling close to a critical value. We expect that our approach will be used to enhance the sensitivity of synthetic bio-sensing networks.

1. Introduction

Synthetic biology involves the design and construction of new biological parts, devices, and systems, as well as the re-design of existing, biological systems for useful purposes [1]. A major application area of synthetic biology is biosensing [2]: engineering systems that enable cells to sense signals and elicit appropriate, predetermined responses. Such biosensing modules are crucial for many of the goals of synthetic biology to be achieved, from controlling bacterial behaviour [3] to the efficient delivery of drugs [4]. Most often biosensing systems are based on natural processes, such as cell signalling and gene regulation, which the cell has evolved to sense environmental changes and regulate its behaviour and phenotype. Biochemical reaction networks are at the heart of these processes, hence stochastic effects and cell-to-cell heterogeneity limits their capacity to transfer information [5, 6]. Therefore, from an engineering perspective a major challenge is how to design a reliable synthetic system using inherently unreliable components. In this article we develop a generic framework for

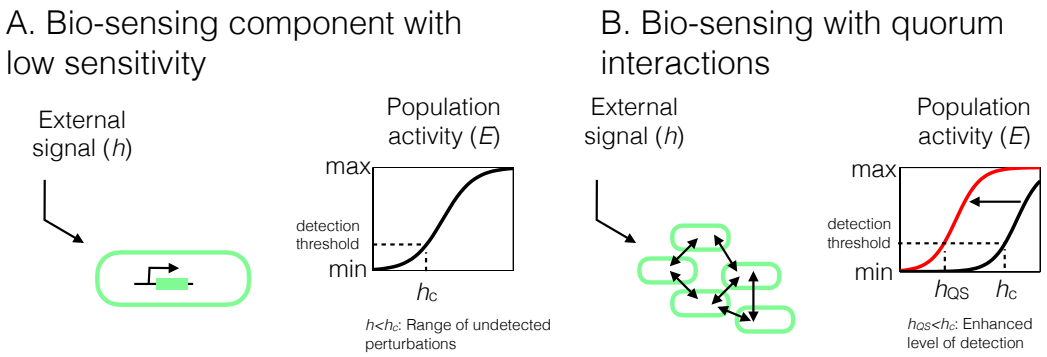

Figure 1. Increasing the sensitivity of a synthetic bio-sensing network. An engineered network responds to an environmental signal h by producing a molecular probe (E). (A) Parameters in the system dictate the sensitivity of the response, i.e. the range of signal values over which the system produces a detectable response. (C) Interactions due to cellular communication (quorum sensing) can be used to increase the sensitivity of the system.

increasing the reliability of a synthetic multicellular biological system by tuning the cell-cell interactions (which can be done by e.g. controlling the density of a bioreactor).

Let us imagine a population of cells that are engineered to detect an environmental input h and produce a molecular probe (E) in response. For the sake of simplicity we assume that the molecular readout is produced through a single catalytic reaction, affected by h, and degraded through a first order reaction. We model the dynamics of the system using a stochastic *birth–death process*:

$$\text{Production:} \quad E \xrightarrow{g(h)} E+1; g(h) = \frac{g_0 h}{K_h + h};$$

$$\text{Degradation:} \quad E \xrightarrow{r(E)} E-1; r(E) = r_0 E,$$

where parameters r_0, g_0 and K_h govern the *propensities* of the two reactions—or how densely these reaction events occur over a time interval. The *Chemical Master Equation*, describing the dynamics of the probability distribution of the cellular responses is given by:

$$\frac{dP(E,t)}{dt} = (\mathbb{E}^{-1} - 1)\frac{g_0 h}{K_h + h} P + (\mathbb{E}^{+1} - 1) r_0 E P, \tag{1}$$

where $\mathbb{E}$ is the step operator, i.e., $\mathbb{E}^a f(x) = f(x+a)$.

From the equation above we derive the population-average, steady-state response of the system $\langle E \rangle = \frac{g_0}{r_0}\frac{h}{K_h+h}$ [7], which for small values of the input, $h \ll K_h$, becomes $\langle E \rangle \approx \frac{g_0 h}{r_0 K_h}$. Therefore, parameter K_h dictates how sensitive the system is to small input perturbations. Assuming that the input can be written as $h = \bar{h} + h_{noise}$, where $\bar{h}$ represents the true signal, and h_{noise} is a zero-mean noise term, often one seeks a system where K_h is large enough to filter out noise ($K_h > \sqrt{\langle h_{noise}^2 \rangle}$) but small enough to allow strong responses to small changes in $\bar{h}$. However, the intrinsic sensitivity of many naturally occurring components, used in biosensing applications, is hard to tune and therefore poses an obstacle

for their use in applications. Our goal is to develop alternative network designs that allow one to circumvent the limitations of the individual components to enhance the overall sensitivity of a biosensing system.

Hence, we propose and study a synthetic gene regulatory system that enables a population of cells to detect with increased sensitivity changes in the external environment. The system is based on cellular communication, also known as quorum sensing (Fig. 1C). In brief, the network consists of two mutually repressing, quorum sensing modules. Each module produces signalling molecules that diffuse across the cell membrane and up-regulate the expression of their cognate module while down-regulating the expression of the non-cognate one. After suitable coarse-graining the state of a cell can be assigned two possible values, corresponding to the predominance of one of the two modules (i.e. ± 1). We perform a statistical mechanical analysis of this system for a population of cells uniformly distributed in two dimensions. The dynamics of the signalling molecules leads to a coupling of nearby cells and the behaviour of the population undergoes a dynamics similar to the Ising model for ferromagnetism [8, 9, 10]. The strength of the coupling can be characterised by a single effective parameter and for values of the coupling parameter close a critical value the behaviour of the population of cells exhibits highly sensitive response to small changes in the environmental variables.

2. Methods

2.1. Synthetic network design

The proposed network consists of two mutually repressing, *Quorum Sensing* (QS) modules. Each module incorporates a *synthetase* (E_1 and E_2) gene under the control of a synthetic promoter. In natural QS systems, synthetase enzymes produce small diffusible (signalling) molecules (here denoted by A_1 and A_2), which bind to *receptor* proteins and activate them. Active receptors are transcriptional activators of the synthetases, giving rise to a positive feedback loop—hence, QS signalling molecules are often referred to as *autoinducers* [11]. The design we propose here, uses synthetic promoters that would enable receptor proteins to function as transcriptional repressors of the non-cognate genes as well. Moreover, one of the promoters (e.g. the one corresponding E_1) is under the control of the external signal of interest. Fig. 2A gives a schematic illustration of the key interactions in the proposed synthetic network.

Positive feedback within each QS module and mutual inhibition between them suggest that the network will function as a toggle switch [12]. This motif produces a bistable expression profile, where one module is active at any time, and switching between modules occurs stochastically in time due to random fluctuations (Fig. 2B). At the population level, QS correlates cellular responses, much like spins in an Ising model (Fig. 2C). The presence of the external signal should result in a bias towards the corresponding state, which will be amplified at the population level given that coupling between cells is appropriately tuned.

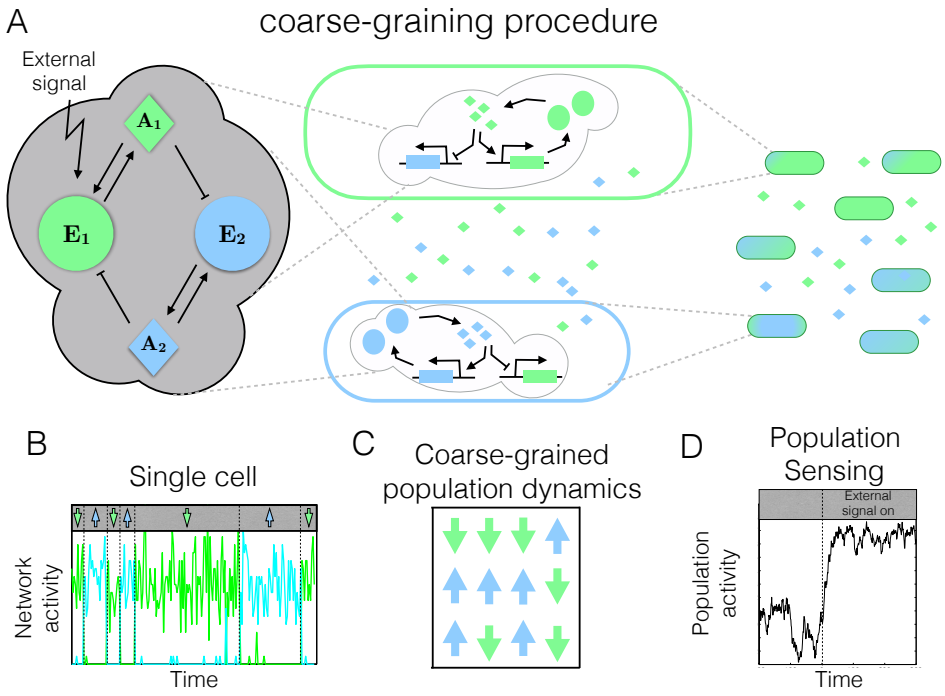

Figure 2. Schematic illustration of the proposed biosensing network. (A) The network consists of two mutually repressing quorum sensing modules. Each module incorporates a gene coding for an enzyme ($E_{1/2}$) that produces quorum sensing molecules ($A_{1/2}$). These small, diffusible molecules bind to receptor proteins and activate the expression of their cognate enzyme while repressing the expression of the non-cognate one. The external signal controls the expression of only on module (e.e., E_1). (B) At the single cell level, the network behaves as a toggle switch (C) After suitable coarse-graining, the population can be represented as a spin lattice, with each spin corresponding to the state of each cell. (D) Tuning the coupling between cells results in sensitive population wide responses even to small levels of external stimulation.

2.2. Model formulation

We formulated a simplified model of the network proposed above and used it to study the single cell and population dynamics. Vector $X = (E_1, E_2, A_1, A_2)$ denotes the state of the network, that is the levels of the enzymes and the signalling species within a cell. The state of the entire cellular population is denoted by $\mathcal{X} = \{X_i\}$ where individual cells are indexed by integer i. The chemical Master Equation describing the dynamics of

$$P(\{x_i\}, t) \equiv P\left(\mathcal{X} = \{x_i\}, t | \mathcal{X} = \{x_{i,0}\}, 0\right),$$

the probability to find the population at state $\{x_i\}$ at time t having started at state $\{x_{i,0}\}$, is given by:

$$\frac{dP(\{x_i\}, t)}{dt} = \sum_{\text{reaction } j} \sum_{\text{cell } k} \left[\mathbb{E}^{\nu_j^k} - 1\right] a_j^k P + \sum_{\text{reaction } j} \sum_{\text{neighbours } \{k,l\}} \left[\mathbb{E}^{\mu_j^{k,l}} - 1\right] b_j^{k,l} P, \tag{2}$$

Biochemical reactions within cell k			
Index j	**Reaction stoichiometry,** $\mathcal{X} \to \mathcal{X} + \nu_j^k$	**Propensity,** $a_j^k(\mathcal{X})$	**Description**
1	$E_1^k \to E_1^k + 1$	h'	externally stimulated production of enzyme E_1, $h' = \frac{g_0 h}{K_h + h} \approx g_0 h / K_h$ assuming $h \ll K_h$.
2	$E_1^k \to E_1^k + 1$	$f(A_1^k, A_2^k)$	regulated production of enzymes E_1 and E_1:
3	$E_2^k \to E_2^k + 1$	$f(A_2^k, A_1^k)$	$f(x,y) = \frac{\beta K^2 + \alpha x^2}{K^2 + x^2 + y^2}$.
4	$E_1^k \to E_1^k - 1$	$\delta \cdot E_1^k$	degradation of enzymes E_1 and E_2.
5	$E_2^k \to E_2^k - 1$	$\delta \cdot E_2^k$	
6	$A_1^k \to A_1^k + 1$	$\alpha_A \cdot E_1^k$	production of signalling molecules.
7	$A_2^k \to A_2^k + 1$	$\alpha_A \cdot E_2^k$	
8	$A_1^k \to A_1^k - 1$	$\delta_A \cdot A_1^k$	degradation of signalling molecules.
9	$A_2^k \to A_2^k - 1$	$\delta_A \cdot A_2^k$	
Transport of signalling molecules from cell k to neighbouring cell l			
Index j	**Reaction stoichiometry,** $\mathcal{X} \to \mathcal{X} + \mu_j^{k,l}$	**propensity** $b_j^{k,l}(\mathcal{X})$	**Description**
1	$(A_1^k, A_1^l) \to (A_1^k - 1, A_1^l + 1)$	$c \cdot A_1^k$	exchange of signalling molecules
2	$(A_2^k, A_2^l) \to (A_2^k + 1, A_2^l - 1)$	$c \cdot A_2^l$	

Table 1. List of reactions involved in the the biochemical network. All reactions (indexed by j) are listed along with their corresponding propensities (a_j, b_j), and how they affect the state of the system $\mathcal{X}$ (v_j, μ_j).

where $\mathbb{E}$ is the step operator, i.e., $\mathbb{E}^{\{a_i\}} f(\{x_i\}) = f(\{x_i + a_i\})$ and all reactions (indexed by j) along with their corresponding propensities (a_j, b_j) and how they affect the state of the system (stoichiometries v_j, μ_j) are listed in Table 2.1. Note that in Eq. 2 we split reactions into two sets: the first set includes all reactions that occur intracellularly, while the second set includes reactions involving exchange of signalling molecules between cells.

For the sake of clarity we choose to study the dynamics of the system in terms of $\tilde{X} = (S, D, S_A, D_A)$, where S is the sum of the levels of the two enzymes, i.e., $S = E_1 + E_2$;

Virtual reactions within cell k		
Index j	**Reaction stoichiometry, $\tilde{\mathcal{X}} \to \tilde{\mathcal{X}} + \tilde{\nu}_j^k$**	**propensity, $\tilde{a}_j^k(\tilde{\mathcal{X}})$**
1	$(S^k, D^k) \to (S^k + 1, D^k + 1)$	$h' + f(\frac{S_A^k + D_A^k}{2}, \frac{S_A^k - D_A^k}{2})$
2	$(S^k, D^k) \to (S^k + 1, D^k - 1)$	$f(\frac{S_A^k - D_A^k}{2}, \frac{S_A^k + D_A^k}{2})$
3	$(S^k, D^k) \to (S^k - 1, D^k - 1)$	$\delta \cdot \frac{S^k + D^k}{2}$
4	$(S^k, D^k) \to (S^k - 1, D^k + 1)$	$\delta \cdot \frac{S^k - D^k}{2}$
5	$(S_A^k, D_A^k) \to (S_A^k + 1, D_A^k + 1)$	$\alpha_A \cdot \frac{S^k + D^k}{2}$
6	$(S_A^k, D_A^k) \to (S_A^k + 1, D_A^k - 1)$	$\alpha_A \cdot \frac{S^k - D^k}{2}$
7	$(S_A^k, D_A^k) \to (S_A^k - 1, D_A^k - 1)$	$\delta_A \cdot \frac{S_A^k + D_A^k}{2}$
8	$(S_A^k, D_A^k) \to (S_A^k - 1, D_A^k + 1)$	$\delta_A \cdot \frac{S_A^k - D_A^k}{2}$
Transfer from cell k to neighbouring cell l		
Index j	**Reaction stoichiometry, $\tilde{\mathcal{X}} \to \tilde{\mathcal{X}} + \tilde{\mu}_j^{k,l}$**	**propensity, $\tilde{b}_j^{k,l}(\tilde{\mathcal{X}})$**
1	$(S_A^k, D_A^k, S_A^l, D_A^l) \to (S_A^k - 1, D_A^k - 1, S_A^l + 1, D_A^l + 1)$	$c \cdot \frac{S_A^k + D_A^l}{2}$
2	$(S_A^k, D_A^k, S_A^l, D_A^l) \to (S_A^k - 1, D_A^k + 1, S_A^l + 1, D_A^l - 1)$	$c \cdot \frac{S_A^k - D_A^l}{2}$

Table 2. List of reactions involved in the the biochemical network. Reaction stochiometries and propensities are presented in the context of the transformed system, $\mathcal{X}'$ (see main text).

D is the difference in the corresponding levels, i.e., $D = E_1 - E_2$; and S_A, D_A are defined similarly in terms of the signalling molecules A_1 and A_2. Table 2 summarises all reactions under this linear transformation of the state variables. We use $\tilde{\mathcal{X}}$ to denote the transformed population state and note that the chemical master equation describing the dynamics of $P(\tilde{\mathcal{X}}, t) \equiv P(\tilde{\mathcal{X}}, t|\tilde{\mathcal{X}}_0, 0)$ would be equivalent to Eq. 2.

2.3. Stochastic simulations

We simulate the coarse-grained system using a kinetic Monte-Carlo scheme [13] (the Gillespie algorithm [14, 15]). For all our simulations we use a square array of 50×50 nodes ($N = 2500$) with periodic boundary conditions. We study systems where initially the effective potentials $U_\pm$ and external signal h' have been tuned so that H (see Eq. 7) is close to zero. Finally, time is measured in units of $1/k_0$, the reciprocal of the basal transition rate between the two states when there is no coupling $J_1 = 0$ and no signal $H = 0$.

3. Results

3.1. Single cells behave like bistable switches

Here, we focus on the dynamics of a single isolated cell, which corresponds to the case where the rate of molecular exchange between cells is set to zero, i.e. $c = 0$. In this case cells behave independently of each other, hence it suffices to study the dynamics of $\tilde{X} = (S, D, S_A, D_A)$. Making the ansatz that $\tilde{X}$ can be written as the sum of a macroscopic part and a random

fluctuating part, $\tilde{X}(t) = \Omega\tilde{\mathcal{S}}(t) + \Omega^{1/2}\Xi(t)$, we derive from Eq. 2 the macroscopic behaviour of the model [7]

$$\frac{d\tilde{\mathcal{S}}}{dt} = M \cdot A(\tilde{\mathcal{S}}) \tag{3}$$

where M is the (4×9) stoichiometric matrix and A is the (9×1) propensity vector (see Tbl. 2).

The macroscopic behaviour is particularly instructive in the limit of strong regulation ($K \to 0$) and in the absence of external stimulation ($h = 0$). In this limit, the system exhibits two stable solutions—corresponding to $D, D_A > 0$ and $D, D_A < 0$—and an unstable one ($D = D_A = 0$). Quantities S, and S_A always attain a unique steady state value irrespective of the steady state of D and D_A. The macroscopic analysis guides our intuition about the stochastic dynamic behaviour of the system. In particular, we expect that for sufficiently long times ($t \gg 1/\delta$), the system will flip between the two meta-stable basins of attractions, owing to random fluctuations.

To strengthen our intuition we study the stochastic dynamics of a coarse grained model, which we obtain for sufficiently long times. Our coarse graining procedure involves decomposing the distribution P as follows:

$$P(\tilde{X}, t) = P(S, D, S_A, D_A, t) = P_1(D, t) \cdot P_2(D_A, t|D) \cdot P_3(S, S_A, t|D, D_A).$$

For sufficiently long times, $t \gg 1/\delta$, allowing S to settle to its steady state, the third component becomes stationary: that is, P_3 becomes narrowly peaked around the macroscopic steady state values S^{ss}, S_A^{ss}, which are independent of t, D, and D_A (see Appendix). Also, since signalling molecules change at a much faster timescale ($\delta_A \gg \delta$) and adapt rapidly to enzyme levels, one expects that at all times P_2 is narrowly peaked around the macroscopic, quasi steady-state implied by the value of $D(t)$. Under the above assumptions the rate of change of P becomes

$$\frac{dP(\tilde{X}, t)}{dt} = \frac{dP_1}{dt} \cdot P_2 \cdot P_3.$$

Replacing the above in Eq. 2 and summing over S, S_A, D_A we obtain a *birth–death process* approximating the dynamics of the system:

$$\begin{aligned}\frac{dP_1(D = n, t)}{dt} = {} & g_{n-1}P_1(n-1, t) + r_{n+1}P_1(x+1, t) \\ & - [g_n + r_n]\, P_1(n, t),\end{aligned} \tag{4}$$

where g (birth rate) and r (death rate) are given by

$$\begin{aligned} g_n &= h' + f\left(\frac{\alpha_A}{\delta_A}\frac{S_{ss}+n}{2}, \frac{\alpha_A}{\delta_A}\frac{S_{ss}-n}{2}\right) + \delta \cdot \frac{S_{ss}-n}{2}, \\ r_n &= f\left(\frac{\alpha_A}{\delta_A}\frac{S_{ss}-n}{2}, \frac{\alpha_A}{\delta_A}\frac{S_{ss}+n}{2}\right) + \delta \cdot \frac{S_{ss}+n}{2}, \end{aligned}$$

$S^{ss} = \frac{\alpha}{\delta}$ is the macroscopic steady state value of S and function f along with all rate constants are defined in Tbl. 2.1 The stationary distribution of Eq. 4 can be written as

$P_1^{ss}(D=n) \propto \exp[-U_0(n)]$, where

$$U_0(n) = \begin{cases} \sum_{j=0}^{n-1} [-\log g_j + \log r_{j+1}] & n \geq 0, \\ \sum_{j=n}^{-1} [\log g_j - \log r_{j+1}] & n < 0. \end{cases} \quad (5)$$

The potential U_0 has two minima: U_+ at value $D = n_+ > 0$ and U_- at $D = n_- < 0$, with a peak (U_b) separating them at $D = n_0$. For example, in the absence of external stimulation ($h = 0$), one obtains $n_\pm = \pm\frac{\alpha}{\delta}$ and $n_0 = 0$. External stimulation $h > 0$ tilts the potential towards positive values, hence biasing the stationary distribution. Equation 4 allows us to calculate the rates of hopping between the two meta-stable states as the mean first passage time between the two minima. In particular, the mean first passage time from n_- to n_+ is $\tau = \left\{\sum_{-\infty}^{n_0} P_1^s(n)\right\} \cdot \left\{\sum_{n=n_-}^{n_+} [g_n \cdot P_1^s(n)]^{-1}\right\}$ and, the rate of hopping from the negative to the positive state (r_+) and vice versa (r_-) are (to first approximation) given by [7]:

$$r_\pm = r_0 \cdot \exp\left[U_b - U_\mp\right],$$

where $r_0 = \frac{\delta}{\alpha}\frac{1}{2\pi}$.

3.2. Coarse-grained model of population (mapping to Ising model)

We start our study of the population dynamics by considering the behaviour of a single cell within a fixed, static population, focusing on the behaviour of $P(\tilde{X}_j|\{\tilde{X}_{i\setminus j}\})$. Following the same procedure as the one detailed in the section above, we derive an effective potential

$$U_j(\{y\}) \simeq U_0(y_j) - U_1 \sum_{l \in \text{n.neigb.}(j)} y_l y_j + \dots ,$$

associated with the stationary conditional distribution for the scaled D_j variable, $\hat{D}_j = D_j/S^{ss}$, i.e., $P_1^{ss}(\hat{D}_j = y_j|\{y_{i\setminus j}\}) \propto \exp[-U_j(\{y\})]$, and also dictating the switching rates of the approximating telegraph process. We note that to first approximation the potential is a function of y_j and its nearest neighbours, y_l, with the first term U_0 given by Eq. 5 and parameter $U_1 = \frac{c}{\delta}$, capturing the strength of the coupling between neighbouring cells.

The *many-particle* dynamics for the full population of cells can be translated into a one-step process in in a high dimensional space $\mathbf{y} = (y_1, y_2, \dots, y_N)$ where N is the number of cells in the population. The dynamics can be further simplified into a model of hopping between the two minima of each cell i. To do so we set $y_i = y_0 + \sigma_i \cdot d_i$, where y_0 is the position of the peak separating the two minima in U_j, $d_i = \text{abs}(y_i - y_0)$ and $\sigma_i = \text{sgn}(y_i - y_0) = \pm 1$, and replace $P_1(\{y_i\}, t) = P_{1,1}(\{\sigma_i\}, t) \cdot P_{1,2}(\{d_i\}, t|\{\sigma_i\})$. For times longer than the times needed for ys to equilibrate in each well $P_{1,2}(\{d_i\}|\{\sigma_i\})$ becomes effectively stationary and hence:

$$\frac{dP_{1,1}[\{\sigma_i\}]}{dt} = \sum_{\{\sigma_n\} \in \{\{\sigma_i\} - \uparrow\downarrow\}} k_{\{\sigma_n\}\to\{\sigma_i\}} P_{1,1}[\{\sigma_n\}] - k_{\{\sigma_i\}\to\{\sigma_n\}} P_{1,1}[\{\sigma_i\}] \ , \quad (6)$$

where the sum is over all states $\{\sigma_n\}$ which differ from $\{\sigma_i\}$ by *one* transition between the states of a *single* node and $k_{\{\sigma_n\}\to\{\sigma_i\}}$ denotes the corresponding transition rate. The transition

rate for a transition where a node i that is in state σ_i (either 1 or -1) switches to $-\sigma_i$ is given by

$$k = k_0 \exp\left(H\sigma_i + J_1 \sum_{j \in \text{n.neigh}(i)} \sigma_i \sigma_j \right) = k_0 e^{-\Delta E} \ , \tag{7}$$

where, $J_1 = U_1$ and $H = h$ measures the presence of the external environment (and possibly other factors or chemical species) that affects the equilibrium between the $\pm$ states. The rate k_0 is the inverse of the timescale for the signalling molecules to diffuse a length scale corresponding to the coarse-graining scale, L, and the class of models we consider here are valid only for systems of size much greater than L. We can give estimates of (lower bounds on) the lengthscale, L, in terms of the density of cells, ρ_{cells}. In a bioreactor, assuming bulk conditions, we have $L \sim \rho_{cells}^{-1/3}$, or $L \sim h^{-1/2}\rho_{cells}^{-1/2}$ assuming a biofilm of height h; and the associated timescale of diffusion is given by L^2/D, where D is the diffusion constant of the signalling molecules—roughly 10^{-9}m^2/s for 1nm-sized molecules at 25°C. For a high cell density environment, such as a biofilm, where L is limited by the size of the cells ($\sim 1\mu$m), one obtains an approximate bound on the rate, $1/k_0 \sim 10^{-3}$sec.

This is mathematically equivalent to the Ising model of a ferromagnet. If we tune h such that $H = 0$, this corresponds to a magnet with *equal* internal energy to each state $(-, +)$ so that an isolated node is equally likely to be in either one of the two possible states. We note that the rate determining parameter ΔE is altered by two factors: (i) the presence of an external signal (field) and (ii) the coupling between nodes mediated through quorum sensing. We emphasise also that for each nearest neighbour j that is changed from the same to the opposite state as i, the rate of transition of the node is increased by a factor e^{+J_1}.

4. Discussion

To examine the effect of quorum sensing on the ability of the population to sense and respond to changes in the concentration of the chemical signal we run a series of computational experiments using the coarse-grained model. Figure 3 shows the response of a single copy of the system—quantified as the fraction of the nodes in the active $(+)$ state—to a stepwise increase in the concentration of the chemical signal. Initially, each node in the lattice is initialised randomly and the system is allowed to reach steady state in the absence of external stimulation ($h = 0$). At $t = 0$ a step-change in the signal is introduced (setting $H = 0.0316$) and the state of the system is recored up to time $t = 200$. In the absence of coupling (quorum sensing) the system's response is weak. As the coupling is increased the magnitude of the system response to the signal increases monotonically. Stronger coupling gives rise to longer range interactions between nodes in the lattice, giving rise to a strong population-wide response when the signal is introduced.

Figure 4 illustrates the average response of the system to various intensities of external stimulation as a function of time. Here, external stimulation is applied at $t = 0$ to a randomly initialised lattice and averaging is performed over 200 independent runs. We focus on the longtime response of the system to an applied signal. With cell communication, the response

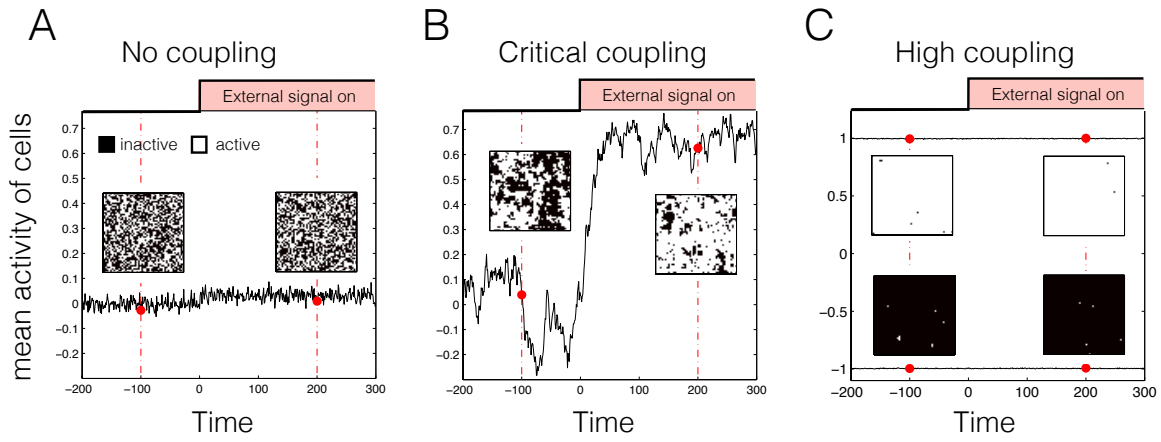

Figure 3. Population responses to a stepwise change of the chemical signal. The mean activity cells over the lattice is plotted as a function of time when (A) there is no intercellular coupling ($J_1 = 0$), (B) the coupling strength is close to the critical value, J_1^* ($J_1 = 0.4$ with $J_1/J_1^* = 0.91$), and (C) the coupling strength is high ($J_1 = 0.8$ with $J_1/J_1^* = 1.82$). The chemical signal is introduced at time $t = 0$ by setting $H = 0.0316$. Insets illustrate the state of each site (S_i) in the lattice before ($t = -100$) and after ($t = 200$) the signal is introduced . Active and inactive sites are shown as white and black squares respectively. Data we collected from a single run of the coarse grained model using a 50×50 lattice with periodic boundary conditions. Time is measured in units of $1/k_0$ the reciprocal of the basal transition rate between the two states when there is no coupling $J_1 = 0$ and no signal $H = 0$.

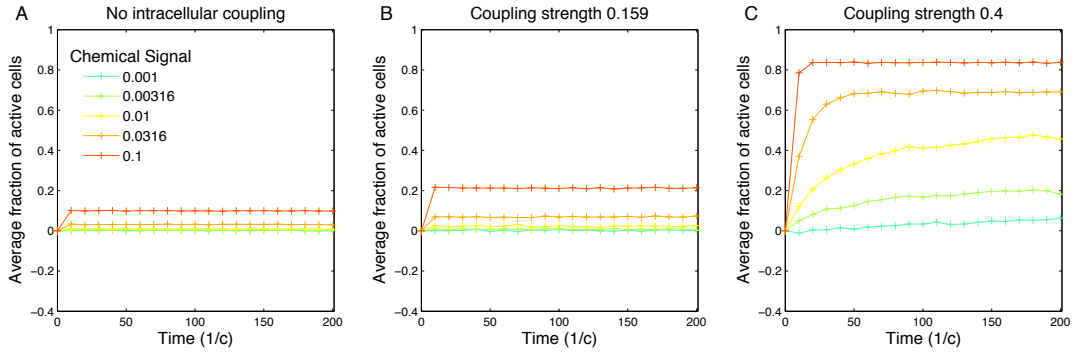

Figure 4. Average population response to a stepwise change in the concentration of the chemical signal. The average fraction of active sites as a function of time for different magnitudes of the step change (coloured lines) and for different strengths of intercellular coupling. (A) No intercellular coupling ($J_1 = 0$), (B) coupling strength $J_1 = 0.159$ and (C) coupling strength $J_1 = 0.4$. The data shown here were generated using a 50×50 lattice with periodic boundary conditions and averaging was performed over 200 independent runs. Time is measured in units of $1/k_0$, the reciprocal of the basal transition rate between the two states when there is no coupling $J_1 = 0$ and no signal $H = 0$.

of the population is as discussed above stronger than in populations without communication. It is however interesting to study its sensitivity to small values of signal as the coupling is increased, there one finds that the sensitivity first increases, then however beyond a critical

value it decreases again. The sensitivity is quantified by the *susceptibility* of the system to external stimulation, defined by measuring the relative change in the magnitude of the response to changes in the applied signal. For uncoupled systems, this shows linear behaviour independent of the applied signal while for coupled systems it shows non-linear behaviour. In particular for specific values of the coupling constant, J_1 close to a critical value, the sensitivity of the system becomes greatly enhanced by several orders of magnitude. We quantify the susceptibility of the system to external stimulation change by measuring the change of the magnitude of the response with respect to the change in the external stimulation as the coupling parameter approaches the critical value. Figure 5 illustrates the the strong nonlinear behaviour of the susceptibility as a function of coupling parameter when the system is close to criticality. The susceptibility diverges as power law of the difference of the coupling parameter from its critical value as one approaches the critical value of the couplings.

Finally we close with a discussion of parameters and how they may be optimised. The response is most sensitive for the background signal close to zero and the coupling close to a critical value so it is interesting to consider how that may be engineered. A natural way to tune the coupling is to control the number density of cells which will change the rates of diffusion of the active molecules between cells and hence the communication between nearby cells. The coupling can also be tuned by varying properties of the buffer that the cells are growing in which will also change the rates of diffusion and hence the cell-cell communication. In addition it can also effectively be changed by varying the amount of 'noise' or fluctuations in the chemical reaction. These will in general be due both to thermal fluctuations as well as fluctuations in the copy number of the chemical species. The background signal can be kept close to zero by tuning the reaction rates within the cells. All of these requirements seem feasible within the current parameters of modern molecular biology [16].

5. Appendix

5.1. Quasi steady state approximation for the macroscopic system

In our analysis of the macroscopic behaviour of the system (see Eq. 3) we assume that the dynamics of the signalling species A_1 and A_2 are sufficiently faster than those of the enzymes E_1 and E_2. This assumption allows us to simplify the macroscopic system using the quasi-steady-state approximation (QSSA). Denoting the macroscopic concentration of the species with $m_{A_1}, m_{A_2}, m_{E_1}, m_{E_2}$, the QSSA approach involves: setting $\frac{dm_{A_1}}{dt} = \frac{dm_{A_2}}{dt} = 0$; solving these equations for the quasi-steady states $m_{A_1}^{qss}$ and $m_{A_2}^{qss}$; and substituting these values into the equations for m_{E_1} and m_{E_2}. The simplified system takes the form:

$$\frac{dm_{E_1}}{dt} = h' + f\left(m_{A_1}^{qss}, m_{A_2}^{qss}\right) - \delta m_{E_1},$$
$$\frac{dm_{E_2}}{dt} = + f\left(m_{A_2}^{qss}, m_{A_1}^{qss}\right) - \delta m_{E_2},$$

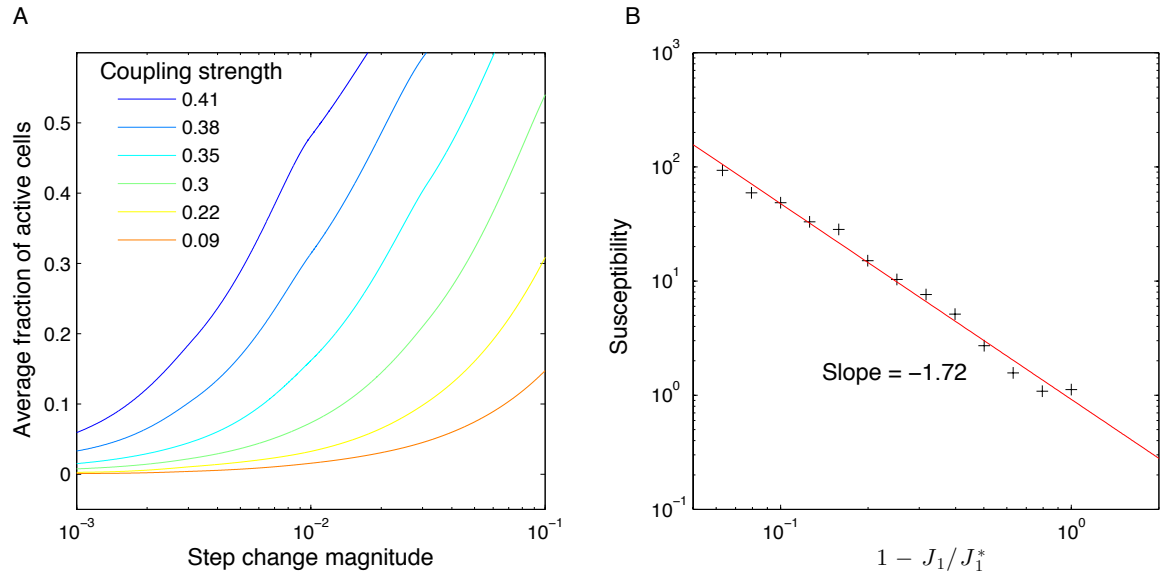

Figure 5. The effect of intercellular coupling on the average steady-state population response to a stepwise increase in the concentration of the chemical signal. (A) The average steady-state population response is shown as a function of the applied change for different coupling strengths (coloured lines). Results shown are averages over 200 independent runs. (B) The change of the magnitude of the response with respect to the applied change is plotted a function of distance from the critical value. The 'susceptibility' exhibits highly nonlinear behaviour as the coupling parameter approaches the critical value. The data shown were generated using a 50×50 lattice with periodic boundary conditions.

where $m_{A_1}^{qss} = m_{E_1}\alpha_A/\delta_A$ and $m_{A_2}^{qss} = m_{E_2}\alpha_A/\delta_A$. Rewriting the above equations in terms of $m_S = m_{E_1} + m_{E_2}$ and $m_D = m_{E_1} - m_{E_2}$ we obtain:

$$\frac{dm_D}{dt} = h' + f\left(\frac{m_S + m_D}{2}\frac{\alpha_A}{\delta_A}, \frac{m_S - m_D}{2}\frac{\alpha_A}{\delta_A}\right) - f\left(\frac{m_S - m_D}{2}\frac{\alpha_A}{\delta_A}, \frac{m_S + m_D}{2}\frac{\alpha_A}{\delta_A}\right) - \delta m_D,$$

$$\frac{dm_S}{dt} = h + f\left(\frac{m_S + m_D}{2}\frac{\alpha_A}{\delta_A}, \frac{m_S - m_D}{2}\frac{\alpha_A}{\delta_A}\right) + f\left(\frac{m_S - m_D}{2}\frac{\alpha_A}{\delta_A}, \frac{m_S + m_D}{2}\frac{\alpha_A}{\delta_A}\right) - \delta m_S.$$

In the limit of strong regulation ($K \to 0$) the above equations simplify into

$$\frac{dm_D}{dt} = h' + \frac{2\alpha m_D m_S}{m_D^2 + m_S^2} - \delta m_D,$$

$$\frac{dm_S}{dt} = h' + \alpha - \delta m_S,$$

which for relatively low values of the signal, $h' < \frac{\alpha(\sqrt{5}-1)}{2}$, yield two stable steady state solutions

$$(m_D^{ss,+}, m_S^{ss}) = \left(\frac{\alpha + h}{\delta}, \frac{\alpha + h}{\delta}\right)$$

$$(m_D^{ss,-}, m_S^{ss}) = \left(\frac{-\alpha - \sqrt{\alpha^2 - 4\alpha h - h^2}}{2\delta}, \frac{\alpha + h}{\delta}\right)$$

and an unstable manifold defined by the line $m_D = \frac{-\alpha + \sqrt{\alpha^2 - 4\alpha h - h^2}}{2\delta}$.

Acknowledgements

TBL acknowledges the support of BrisSynBio, a BBSRC/EPSRC Synthetic Biology Research Centre, grant number BB/L01386X/1. MV acknowledges the support of MRC (Strategic Skills Development Fellowship in Biomedical Informatics) and EPSRC via grant number EP/N014391/1

[1] Shankar Mukherji and Alexander van Oudenaarden. Synthetic biology: understanding biological design from synthetic circuits. *Nature Reviews Genetics*, 2009.

[2] Ahmad S Khalil and James J Collins. Synthetic biology: applications come of age. *Nature Reviews Genetics*, 11(5):367–379, 2010.

[3] Gianfranco Fiore, Antoni Matyjaszkiewicz, Fabio Annunziata, Claire Grierson, Nigel Savery, Lucia Marucci, and Mario di Bernardo. In-silico analysis and implementation of a multicellular feedback control strategy in a synthetic bacterial consortium. *ACS Synthetic Biology*, 2016.

[4] M Omar Din, Tal Danino, Arthur Prindle, Matt Skalak, Jangir Selimkhanov, Kaitlin Allen, Ellixis Julio, Eta Atolia, Lev S Tsimring, Sangeeta N Bhatia, et al. Synchronized cycles of bacterial lysis for in vivo delivery. *Nature*, 536(7614):81–85, 2016.

[5] R Cheong, A Rhee, C J Wang, and I Nemenman. Information Transduction Capacity of Noisy Biochemical Signaling Networks. *Science*, 2011.

[6] Margaritis Voliotis, Rebecca M Perrett, Chris McWilliams, Craig A McArdle, and Clive G Bowsher. Information transfer by leaky, heterogeneous, protein kinase signaling systems. *Proceedings of the National Academy of Sciences*, 111(3):E326–E333, 2014.

[7] N G Van Kampen. *Stochastic Processes in Physics and Chemistry*. Elsevier, 2011.

[8] J J Binney, N J Dowrick, A J Fisher, and M E J Newman. *The Theory of Critical Phenomena: An Introduction to the Renormalization Group*. Oxford University Press, 1992.

[9] Yu Shi and Thomas Duke. Cooperative model of bacterial sensing. *Physical Review E*, 58(5):6399–6406, 1998.

[10] TAJ Duke and D Bray. Heightened sensitivity of a lattice of membrane receptors. *Proceedings of the National Academy of Sciences*, 96(18):10104–10108, 1999.

[11] Wai-Leung Ng and Bonnie L Bassler. Bacterial Quorum-Sensing Network Architectures. *Annual Review of Genetics*, 43(1):197–222, 2009.

[12] James J Collins, Timothy S Gardner, and Charles R Cantor. Construction of a genetic toggle switch in Escherichia coli. *Nature*, 403(6767):339–342, 2000.

[13] David P Landau and Kurt Binder. *A Guide to Monte Carlo Simulations in Statistical Physics*. Cambridge University Press, 2009.

[14] D T Gillespie. Exact stochastic simulation of coupled chemical reactions. *The journal of physical chemistry*, 81(25):2340–2362, 1977.

[15] Daniel T Gillespie. Stochastic Simulation of Chemical Kinetics. *Annual Review of Physical Chemistry*, 58(1):35–55, 2007.

[16] W. Weber and M. Fussenegger. *Synthetic Gene Networks: Methods and Protocols*. Methods in Molecular Biology. Humana Press, 2011.